Novel Mechanism of Inhibition by the P2 Receptor Antagonist PPADS of ATP-Activated Current in Dorsal Root Ganglion Neurons

CHAOYING LI
Laboratory of Molecular and Cellular Neurobiology, National Institute on Alcohol Abuse and Alcoholism, National Institutes of Health, Bethesda, Maryland 20892-8115

Li, Chaoying. Novel mechanism of inhibition by the P2 receptor antagonist PPADS of ATP-activated current in dorsal root ganglion neurons. *J. Neurophysiol.* 83: 2533–2541, 2000. The antagonist pyridoxal-phosphate-6-azophenyl-2′,4′-disulfonic acid (PPADS) has been proposed to selectively antagonize the actions of ATP at P2X receptors. Whole cell patch-clamp recording techniques therefore were used to characterize PPADS inhibition of ATP-activated current in bullfrog dorsal root ganglion (DRG) neurons. PPADS, 0.5–10 μM, inhibited ATP-activated current in a concentration-dependent manner with an IC_{50} of 2.5 $\pm$ 0.03 μM. PPADS produced a gradual decline of ATP-activated current to a steady state, but this was not an indication of use dependence as the gradual declining component could be eliminated by exposure to PPADS before ATP application. In addition, ATP-activated current recovered completely from inhibition by PPADS in the absence of agonist. The slow onset of inhibition by PPADS was not apparently due to an action at an intracellular site as inclusion of 10 μM PPADS in the recording pipette neither affected the ATP response nor did it alter inhibition of the ATP response when 2.5 μM PPADS was applied externally. PPADS, 2.5 μM, decreased the maximal response to ATP by 51% without changing its EC_{50}. PPADS inhibition of ATP-activated current was independent of membrane potential between −80 and +40 mV and did not involve a shift in the reversal potential of the current. The magnitude of PPADS inhibition of ATP-activated current was dependent on the duration of the prior exposure to PPADS. The time constants of both onset and offset of PPADS inhibition of ATP-activated current did not differ significantly with changes in ATP concentration from 1 to 5 μM. Recovery of ATP-activated current from PPADS inhibition also exhibited a slow phase that was not accelerated by the presence of agonist and was dependent on the concentration of PPADS. The apparent dissociation rate of PPADS from unliganded ATP-gated ion channels was much greater than the rate of the slow phase of recovery of ATP-activated current from PPADS inhibition. The results suggest that PPADS can inhibit P2X receptor function in a complex noncompetitive manner. PPADS produces a long-lasting inhibition that does not appear to result from open channel block but rather from an action at an allosteric site apparently accessible from the extracellular environment that involves a greatly reduced rate of dissociation from liganded versus unliganded ATP-gated ion channels.

INTRODUCTION

ATP, in addition to its function as an intracellular energy donor, is now recognized as an important neurotransmitter or cotransmitter in both the central and peripheral nervous systems (Ralevic and Burnstock 1998). ATP is released from a variety of cell types, including nerve fibers, upon stimulation and produces diverse effects on many tissues by activation of specific membrane receptors known as P2 receptors (Burnstock 1972, 1978). These receptors have been subdivided further into P2X and P2Y receptors, which have similar agonist potency profiles (P2X: 2-MeSATP $\geq$ ATP $>$ α,β-MeATP; P2Y: 2-MeSATP $\gg$ ATP $>$ α,β-MeATP) (Kennedy and Leff 1995), but differ in their molecular structure and associated transduction mechanisms. P2X receptors are ligand-gated ion channels with two membrane-spanning domains, whereas P2Y receptors are G-protein-coupled receptors with typically seven membrane-spanning domains (Abbracchio and Burnstock 1994; Fredholm et al. 1994).

Ideally, subtype-selective and reversible P2 receptor antagonists would greatly facilitate study of each class of P2 receptor. Unfortunately, the three commonly used P2 receptor antagonists, suramin, an anti-trypanosomal agent; reactive blue 2, an anthraquinone sulfonic acid derivative, and pyridoxal-phosphate-6-azophenyl-2′,4′-disulfonic acid (PPADS), a sulfonic acid derivative, do not meet these criteria. Suramin was introduced by Dunn and Blakeley (1988) as an antagonist of P2 receptor-mediated responses in mouse vas deferens. However, subsequent studies revealed that this agent does not discriminate between the P2X and P2Y subtypes (Kennedy 1990). Reactive blue 2 has been classified as a putative P2Y receptor antagonist that possesses limited selectivity for the P2Y receptor over the P2X receptor (Abbracchio and Burnstock 1994; Kennedy 1990), but recent studies show that it is also an effective antagonist for P2X receptors in rat vas deferens and a number of neuronal preparations (Khakh et al. 1994, 1995; Li et al. 1997a; Trezise et al. 1994). The initial study by Lambrecht et al. (1992) on the action of PPADS on contractile responses of the rabbit vas deferens to α,β-MeATP and to electrical field stimulation led to the classification of PPADS as a P2X receptor antagonist. PPADS does not appear to be selective for P2X receptors, however, as it also has recently been reported to inhibit P2Y receptor-mediated responses in bovine aortic endothelial cells (Brown et al. 1995), guinea-pig taenia coli and rat duodenum (Windscheif et al. 1995).

Recent studies from various neuronal preparations revealed that suramin and reactive blue 2 are not only ineffective in distinguishing subtypes of P2 receptors but also do not discriminate between the P2 receptor and other neurotransmitter-gated receptors. For instance, it has been reported that suramin and reactive blue 2 inhibit radioligand binding to the *N*-methyl-D-aspartate (NMDA) receptor (Balcar et al. 1995) and NMDA-activated current in CNS neurons at concentrations comparable with those required to inhibit ATP responses in P2X receptors (Motin and Bennett 1995;

The costs of publication of this article were defrayed in part by the payment of page charges. The article must therefore be hereby marked "*advertisement*" in accordance with 18 U.S.C. Section 1734 solely to indicate this fact.

Nakazawa et al. 1995; Peoples and Li 1998). In addition, both suramin and reactive blue 2 inhibit GABA-activated ion current in rat hippocampal neurons (Nakazawa et al. 1995). By contrast, PPADS at concentrations up to 100 μM does not affect NMDA-activated current in mouse hippocampal neurons (Peoples and Li 1998) and AMPA- and NMDA-induced increases in action potential firing in rat locus coeruleus neurons (Fröhlich et al. 1996). Over a similar concentration range, PPADS also does not affect GABA-activated ion current in either mouse hippocampal or rat dorsal root ganglion (DRG) neurons (unpublished observations). Thus these observations indicate that, compared with suramin and reactive blue 2, PPADS is the most selective antagonist for P2 receptors and should be a useful tool to study the function of these receptors, such as their involvement in synaptic transmission.

Because the effects of PPADS and its mechanism of action on ATP-activated ion current in neurons have not been well established, the aim of the present study was to characterize the effects of PPADS on ATP-activated current in bullfrog DRG neurons, which are known to possess P2X receptors (Bean 1990; Bean et al. 1990; Li et al. 1997a,b).

METHODS

Isolation of neurons

Freshly isolated neurons from bullfrog DRG were prepared as described previously (Li et al. 1997a,b). Briefly, adult male bullfrogs (*Rana catesbeiana*) were decapitated, and DRGs were dissected rapidly, minced, and dissociated by incubation in trypsin III (0.55 mg/ml) and collagenase 1A (1.1 mg/ml) in Dulbecco's modified Eagle's medium (DMEM) solution (1.38 g DMEM and 0.2 g NaCl dissolved in 100 ml distilled water, pH 7.2, osmolality 260 mmol/kg), at 35°C for 25 min in a water bath shaker. Soybean trypsin inhibitor I-S (1.8 mg/ml) was added to stop trypsin digestion. The care and use of animals in this study was approved by the Animal Care and Use Committee of the National Institute on Alcohol Abuse and Alcoholism (protocol no. LMCN-SP-01) in accordance with National Institutes of Health guidelines.

Whole cell patch-clamp recording

Neurons were observed under an inverted microscope (Diaphot, Nikon, Japan) using phase-contrast optics. Patch-clamp recording of whole cell currents was performed at room temperature using an EPC-7 (List Electronic, Darmstadt, Germany) patch-clamp amplifier connected via a Labmaster TL-1 interface to a computer (Compaq 386/20e). Gigaohm seals were made using borosilicate glass microelectrodes (World Precision Instruments, Sarasota, FL) with tip resistances of 2–4 MΩ, when filled with internal solution. Series resistance in all recordings was $<$5 MΩ and was compensated by 50–70%. Membrane potential was held at $-$60 mV in all experiments, except where indicated. Data were filtered at 3 kHz, displayed on a digital oscilloscope (2090-IIIA, Nicolet Instrument, Madison, WI) and recorded on a chart recorder (2400S, Gould Electronics, Valley View, OH). In experiments measuring the rates of onset and offset (see following text), data were filtered at 3 kHz, recorded on videotape using a VR-10B digital data recorder (Instrutech, Great Neck, NY) connected to a videocassette recorder (Sony SLV-440) and were later refiltered at 1 kHz and acquired at 2 kHz on a computer using pCLAMP software (Axon Instruments, Foster City, CA).

The patch-pipette (internal) solution contained (in mM) 110 CsCl, 2 $MgCl_2$, 0.4 $CaCl_2$, 4.4 EGTA, 5 HEPES, and 1.5 ATP; pH was buffered to 7.2 using CsOH, and osmolality was adjusted to 240 mmol/kg with sucrose when necessary. The external solution contained (in mM) 117 NaCl, 2 KCl, 2 $CaCl_2$, 2 $MgCl_2$, 5 HEPES, and 10 D-glucose; pH was buffered to 7.2 using NaOH, and osmolality was adjusted to 260 mmol/kg with sucrose. Culture dishes containing neurons were continuously superfused at 1–2 ml/min with normal external solution. Drug solutions were prepared in extracellular medium; addition of PPADS, even at the highest concentration (10 μM) tested, did not appreciably change the pH of the solution. Solutions of ATP, added as the Na^+ salt, were prepared daily.

Drug and agonist solutions were applied by gravity flow using a linear multibarrel array of fused silica tubing (200 μm ID) placed within 100 μm of the cell body. Cells were constantly bathed in extracellular medium flowing from one barrel (flow rate $\sim$3 μl/s), and treatment solutions were applied by opening a valve and moving the barrel array so that the desired solution bathed the cell (10–90% rise time of the junction potential at an open pipette tip was $<$50 ms).

Rapid application of solutions

Measurement of rates of onset and offset of inhibition by PPADS of ATP-activated current (see Fig. 4) was performed using a rapid superfusion system described previously (Li et al. 1997a; Peoples and Li 1998). Briefly, this system consisted of two 300-μm-ID fused silica tubes set at $\sim$30° to each other. Each of these exit tubes was connected to four barrels of 300-μm-ID fused silica tubing glued together in a cylindrical pattern. Each barrel was connected to a reservoir via a solenoid valve (Lee, Westbrook, CT). Solution flowed continuously from one of the two exit tubes, and solutions were changed rapidly by closing and opening solenoid valves to switch the flow between the two exit tubes. Solenoid valves were controlled by computer using locally written software (VDriver; R. W. Peoples) to allow for rapid and precise opening and closing. Using this system, the 10–90% rise time of the junction potential at an open pipette tip was $\sim$2 ms.

Patch-pipette perfusion

Internal perfusion via the patch-pipette was performed using a modification of a pipette perfusion system (ALA Scientific Instruments, Westbury, NY), as described previously (Li et al. 1997b). The time for complete solution exchange was 1–2 min; $\geq$5–6 min were allowed to elapse after the pipette solution was exchanged to permit equilibration of the pipette solution throughout the cell. This technique has been demonstrated to be an effective means of applying substances to the intracellular compartment (Gu and Sackin 1995). The diffusion of PPADS in the interior of the cell was estimated by using the equation

$$\tau_d = 0.6 \cdot R_A \cdot MW^{1/3} \cdot [(C_M/5.91)]^{1.5} \quad (1)$$

where τ_d is the time constant for diffusion in seconds, R_A is access (series) resistance in megaohms, *MW* is the molecular weight of the diffusing substance (PPADS), and C_M is the cell capacitance in picoFarads (Pusch and Neher 1988).

Drugs and chemicals

PPADS was obtained from Research Biochemicals International (Natick, MA), and all other drugs, including reactive blue 2 (Basilen Blue) and ATP (as the sodium salt), were obtained from Sigma Chemical (St. Louis, MO). The salts were purchased from Mallinckrodt (Paris, KY).

Data analysis

Average values are expressed as mean peak currents $\pm$ SE, with *n* equal to the number of cells studied. Data were statistically compared using the Student's *t*-test or ANOVA, as noted. Statistical analysis of concentration-response data were performed using the nonlinear curve-fitting program ALLFIT (DeLean et al. 1978). Values reported

for concentration-response analysis are those obtained by fitting the data to the equation

$$Y = E_{max}/[1 + (EC_{50}/X)^{-n}] \quad (2)$$

where X and Y are concentration and response, respectively, E_{max} is the maximal response, EC_{50} is the concentration yielding 50% of maximal effect (EC_{50} for activation, IC_{50} for inhibition), and n is the slope factor.

The time constants of onset and offset of inhibition by PPADS of ATP-activated current were determined by fitting the data to a single exponential function using the program NFIT (Island Products, Galveston, TX).

RESULTS

Inhibition of PPADS on ATP-activated current

Extracellular ATP can activate a nondesensitizing inward current in bullfrog DRG neurons by activation of a type of P2X receptor (Bean 1990; Bean et al. 1990; Li et al. 1997a,b). The inhibition of ATP-activated inward current by PPADS in these neurons is illustrated in Fig. 1. As shown in Fig. 1*A*, the simultaneous application of PPADS, at a concentration of 2.5 μM, and ATP, at a concentration of 2.5 μM, slightly reduced the initial peak amplitude of current activated by ATP, followed by a slow decline in current amplitude to a steady-state level, resulting in a peak:steady-state current amplitude ratio of 1.71. Recovery from inhibition by PPADS was complete after 8 min and did not require the presence of agonist. To evaluate whether the slow onset of inhibition of ATP-activated current by PPADS is due to a slow action of PPADS or an action that requires the presence of agonist, as would occur if PPADS acted by enhancing desensitization or by blocking the open channel, the effect on peak ATP-activated current of PPADS applied for 10 s before application of ATP was determined. In the cell shown in Fig. 1*A*, when PPADS alone was applied for 10 s before ATP, the peak:steady-state current amplitude ratio was 1.00. The average values of peak:steady-state ratio were 1.72 ± 0.22 for 2.5 μM PPADS applied simultaneously with ATP and 1.04 ± 0.06 for PPADS applied for 10 s before ATP; these values differed significantly (Student's *t*-test; $P < 0.05$, $n = 5$). In all subsequent experiments, PPADS was preapplied for 5–30 s, unless indicated otherwise (see Fig. 7). Slowly developing inhibition of ATP-activated current by PPADS was observed in all neurons tested ($n = 98$).

PPADS inhibition of ATP-activated current exhibited a clear concentration-dependence. Figure 1*B* shows the average inhibition of 2.5 μM ATP-activated current by PPADS over the range of 0.5–10 μM. The calculated IC_{50} was 2.5 ± 0.03 μM, the slope factor was 1.82 ± 0.05 which is significantly different from 1 (ANOVA, $P < 0.05$), and the maximal effect was 100 ± 6% inhibition. Over the concentration range of 0.5–10 μM, application of PPADS alone did not activate detectable current (data not shown).

Effect of agonist concentration on PPADS inhibition of ATP-activated current

To examine whether the concentration of ATP affects PPADS inhibition, the magnitude of inhibition of ATP-activated current by PPADS was determined at various concentrations of ATP. As shown in Fig. 2*A*, the percentage inhibition

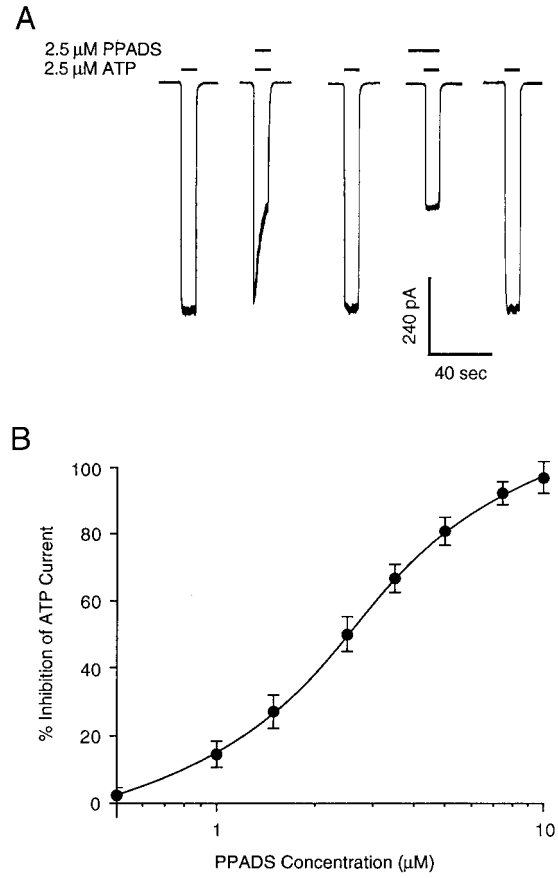

FIG. 1. Inhibition of ATP-activated current by pyridoxal-phosphate-6-azophenyl-2′,4′-disulfonic acid (PPADS). *A*: traces showing currents activated by 2.5 μM ATP and their inhibition by 2.5 μM PPADS. Solid bar above each record indicates time of agonist application in the absence or presence of PPADS, as labeled. Note that the gradual onset of inhibition produced by PPADS applied simultaneously with ATP was eliminated by 10 s preapplication of PPADS. *B*: concentration-response curve for PPADS inhibition of current activated by 2.5 μM ATP. PPADS first was preapplied for 5–30 s depending on PPADS concentration to allow for equilibration (see Fig. 7) and then simultaneously applied with ATP for 4 s. Each point is the average of 4–8 cells; error bars indicate SE. Curve shown is the best fit of the data to the *Eq. 2*. Fitting the data to this equation yielded an IC_{50} of 2.5 ± 0.03 μM, a slope factor of 1.82 ± 0.05, and an E_{max} of 100 ± 6% of inhibition.

by PPADS was not reduced by increasing the concentration of ATP from 1 to 30 μM. Concentration-response analysis (Fig. 2*B*) revealed that PPADS, 2.5 μM, reduced the E_{max} of ATP by 51 ± 0.7% (ANOVA, $P < 0.05$) but did not alter the EC_{50} of ATP (2.6 ± 0.33 μM vs. a control value of 2.5 ± 0.6 μM; $P > 0.05$) or the slope factor of the curve (1.2 ± 0.15 vs. a control value of 1.1 ± 0.24; $P > 0.05$).

Effect of membrane potential on inhibition of ATP-activated current by PPADS

To examine whether inhibition of ATP-gated channels by PPADS was voltage dependent, the amplitude of current activated by 2.5 μM ATP was measured over a range of holding potentials in the absence and presence of 2.5 μM PPADS. As illustrated in Fig. 3*A*, the average inhibition of ATP-activated current by PPADS did not differ significantly at membrane holding potentials between −80 and +40 mV (ANOVA, $P > 0.25$; $n = 5$). In addition, as can be seen from the current-

voltage relationship for 2.5 μM ATP-activated current in the absence and presence of 2.5 μM PPADS (Fig. 3*B*), PPADS did not change the reversal potential of ATP-activated current (Student's *t*-test, $P > 0.1$; $n = 5$).

Kinetics of PPADS inhibition of ATP-activated current

To examine further the mechanism of PPADS action on ATP-gated channels, the onset and offset time constants of inhibition of ATP-activated current by PPADS were measured using rapid solution application. As shown in Fig. 4*A*, in this neuron the rates of onset and offset of inhibition by PPADS in the presence of 2.5 μM ATP were not appreciably different from those observed in the presence of 5 μM ATP. On average, the time constants of onset of PPADS inhibition (τ_{on}) were independent of ATP concentration (ANOVA, $P > 0.25$; $n = 5$) but were highly dependent on PPADS concentration (ANOVA, $P < 0.01$; $n = 5$; Fig. 4*B*). The time constants of offset of PPADS inhibition (τ_{off}), however, were independent of either ATP or PPADS concentration (ANOVA, $P > 0.25$; $n = 5$; Fig. 4*C*).

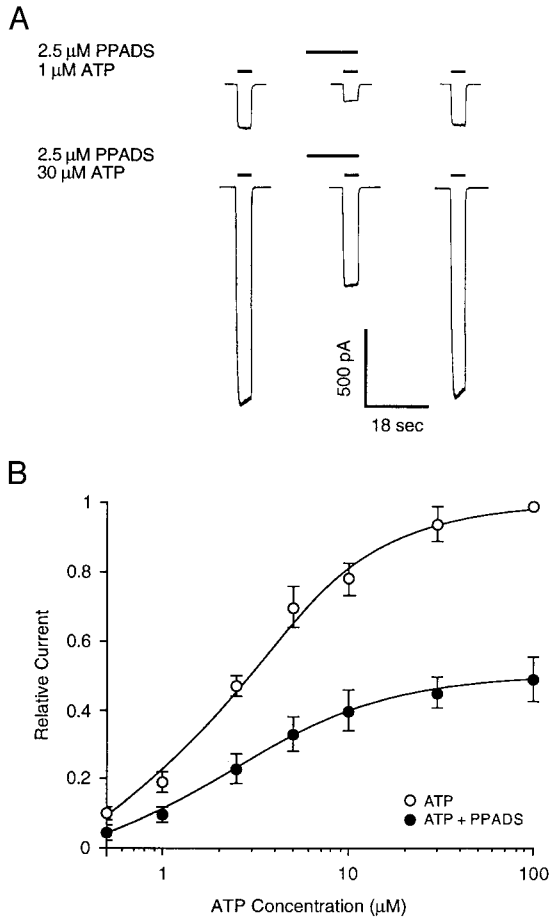

FIG. 2. Effect of ATP concentration on PPADS inhibition of ATP-activated current. *A*: records showing currents activated by 1 μM ATP (*top*) and 30 μM ATP (*bottom*) before, during and after application of 2.5 μM PPADS in a single cell. *B*: graph plotting the relative amplitude of ATP-activated current in the absence (○) and presence (●) of 2.5 μM PPADS as a function of ATP concentration. Amplitude is normalized to the current activated by 100 μM ATP in the absence of PPADS. Each data point is the average current from 5 to 8 cells. Curves shown are the best fits of the data to the *Eq. 2*. PPADS significantly decreased the E_{max} of ATP by 51 ± 0.7% (ANOVA, $P < 0.05$). PPADS was preapplied for 10 s in *A* and *B*.

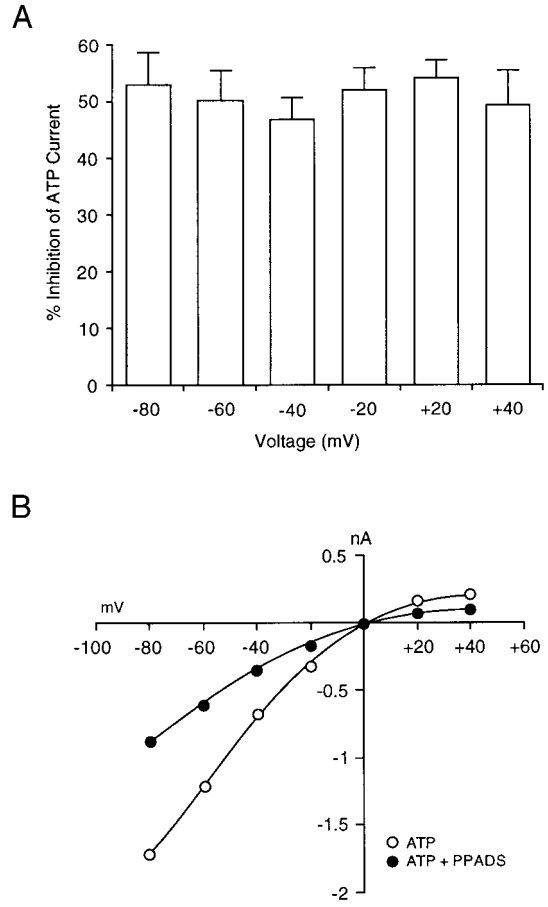

FIG. 3. Effect of membrane potential on inhibition of ATP-activated current by PPADS. *A*: bar graph showing inhibition by 2.5 μM PPADS of current activated by 2.5 μM ATP at membrane potentials from −80 to +40 mV. Percentage inhibition of ATP-activated current by PPADS was not significantly different at the holding potentials shown (ANOVA, $P > 0.25$; $n = 5$). *B*: current-voltage relationship for currents activated by 2.5 μM ATP in the absence (○) and the presence (●) of 2.5 μM PPADS at membrane potentials between −80 and +40 mV in a single cell. Average reversal potential of current activated by 2.5 μM ATP was −1 ± 4 mV in the absence and 1 ± 6 mV in the presence of 2.5 μM PPADS; these values are not significantly different (Student's *t*-test, $P > 0.25$, $n = 5$). In *A* and *B*, membrane potential was held at different levels for ≥1 min before evoking the current, and PPADS was preapplied for 10 s.

Slow phase of recovery of ATP-activated current from PPADS inhibition is not accelerated by the presence of agonist

The records illustrated in Fig. 4*A* suggest the existence of a phase of recovery from PPADS inhibition that is significantly slower than the measured offset rate, as the ATP-activated current did not fully return to control values within 12 s after removal of PPADS. To investigate whether this delayed phase of recovery of ATP-activated current from PPADS inhibition results from a slow exit of PPADS from its site of action in a manner that is accelerated by the presence of agonist, the effect of exposure to agonist on the rate of recovery of ATP-activated current from PPADS inhibition was determined. As shown in Fig. 5, in this neuron 2.5 μM ATP-activated current had fully recovered from inhibition by 2.5 μM PPADS after 8 min. Three additional applications of ATP within this 8-min interval did

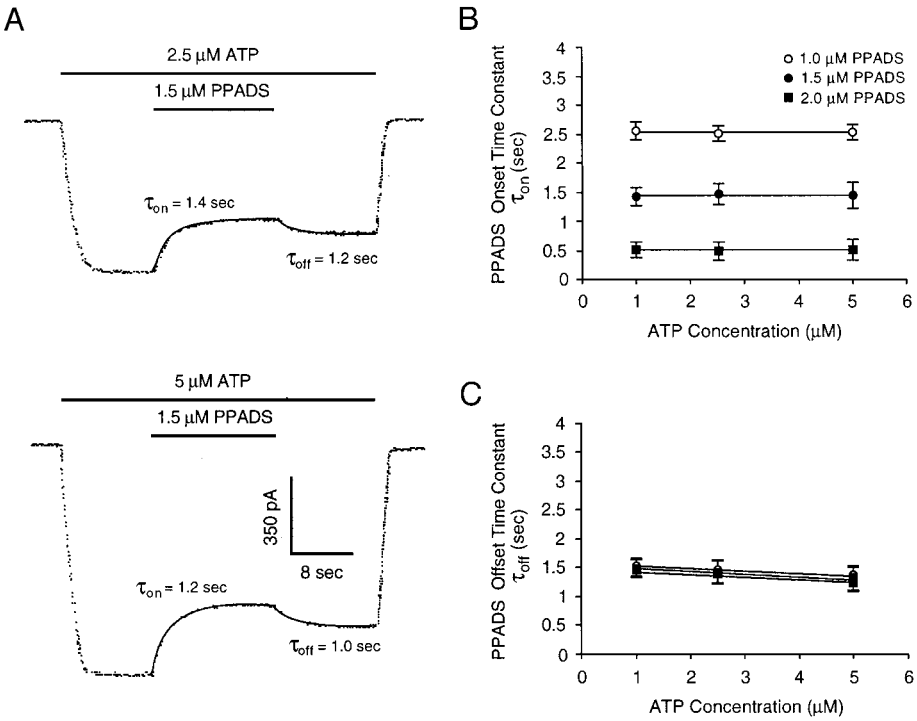

FIG. 4. Measurement of onset and offset time constants of inhibition of ATP-activated current by PPADS. *A*: traces showing currents activated by 2.5 (*top*) and 5 μM (*bottom*) ATP and their inhibition by 1.5 μM PPADS. Both onset and offset of PPADS inhibition were well fitted using single-exponential equations (—). Time constants of onset (τ_{on}) and offset (τ_{off}) values in *A* are those obtained for the records shown. *B*: graph plotting average τ_{on} values as a function of ATP concentration for 1 (○), 1.5 (●), and 2 μM (■) PPADS respectively. Average τ_{on} values were highly dependent on PPADS concentration (ANOVA, $P < 0.01$; $n = 5$) but were independent of ATP concentration (ANOVA, $P > 0.25$; $n = 5$). *C*: graph plotting average τ_{off} values as a function of ATP concentration for 1 (○), 1.5 (●), and 2 μM (■) PPADS respectively. Average τ_{off} values were independent of either PPADS or ATP concentration (ANOVA, $P > 0.25$; $n = 5$).

not result in a more rapid return to control current amplitude. Similar results were obtained in four other neurons.

Effect of patch-pipette application of PPADS on PPADS inhibition of ATP-activated current

The observation that PPADS inhibition of ATP-activated current was gradual in onset might reflect the time required for PPADS to cross the cell membrane and reach an intracellular site of action. To test this possibility, neurons were dialyzed with pipette solutions containing a high concentration of PPADS by using a patch-pipette perfusion technique. The average percentage equilibration of PPADS in the cytoplasm was estimated to be 95 ± 1.4% at the start of recording (5–6 min after establishing whole cell recording mode; $n = 5$). One example of these experiments is shown in Fig. 6. In this neuron, the amplitude of current activated by 2.5 μM ATP was unchanged when the patch pipette was perfused with solution containing 10 μM PPADS. In addition, when the normal patch-pipette solution was replaced by solution containing 10 μM PPADS, the amplitude of inward current activated by 2.5 μM ATP was inhibited to a similar extent by externally applied 2.5 μM PPADS. On average, replacing the normal patch-pipette solution with solution containing 10 μM PPADS did not affect either the amplitude of ATP-activated current (884 ± 52 vs. 923 ± 61 pA, respectively; Student's *t*-test, $P > 0.2$; $n = 5$) or inhibition of ATP-activated current by extracellularly applied 2.5 μM PPADS (51 ± 5 vs. 53 ± 8% inhibition in normal and PPADS-containing patch-pipette solutions, respectively; Student's *t*-test, $P > 0.2$; $n = 5$).

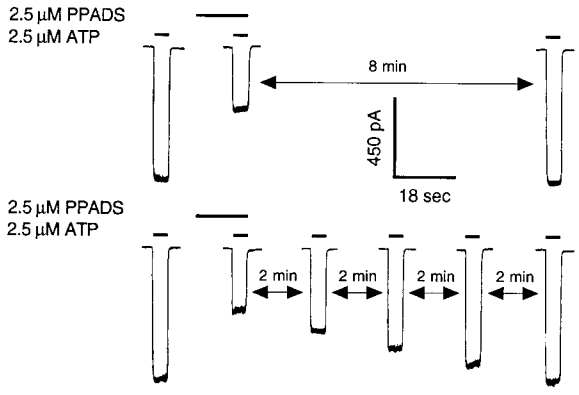

FIG. 5. Slow phase of recovery of ATP-activated current from PPADS inhibition is not accelerated by the presence of agonist. Records of current activated by 2.5 μM ATP in the absence and the presence of 2.5 μM PPADS. Recovery of ATP-activated current from PPADS inhibition was complete after 8 min (*top*); 3 additional applications of ATP within this 8-min interval did not result in a more rapid return to control current amplitude (*bottom*). Records were obtained from a single cell, and PPADS was preapplied for 10 s.

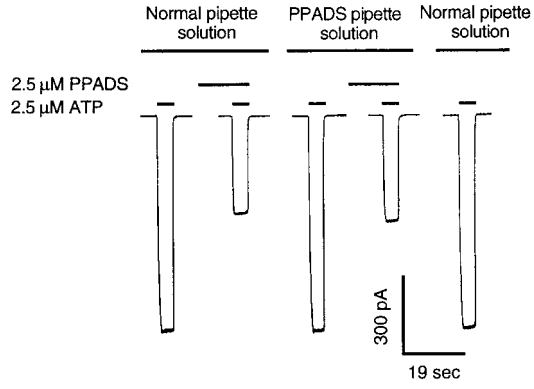

FIG. 6. Effect of intracellular application of PPADS on extracellular PPADS inhibition of ATP-activated current. Records showing current activated by 2.5 μM ATP and its inhibition by 2.5 μM PPADS in normal or 10 μM PPADS-containing patch-pipette solution in the same cell. Note that changing patch-pipette solution from normal to PPADS-containing solution did not affect either ATP-activated current amplitude or PPADS inhibition of ATP-activated current. PPADS was preapplied for 10 s.

Onset of inhibition of ATP-activated current by PPADS in the absence of agonist

To determine the rate of onset of inhibition of ATP-activated current by PPADS in the absence of agonist, PPADS was applied for various periods of time before application of agonist using the protocol shown in Fig. 7*A*. The inhibition of the ATP response relative to control ATP response was plotted against the time period of preincubation with PPADS (Fig. 7*B*). As can be seen, the time required for PPADS to inhibit the response to ATP was dependent on the concentration of PPADS. Fitting the data to a single exponential decay yielded time constants of 16.4 ± 4.5, 9.2 ± 1.7, and 2.9 ± 1.5 s for 1, 1.5, and 2.5 μM PPADS, respectively. These rates of onset were much slower than those observed in the presence of ATP (Fig. 4).

Time course of slow recovery from inhibition of ATP-activated current by PPADS

The rate of the slow phase of recovery of ATP-activated current from inhibition by three concentrations of PPADS also was assessed. One example of these experiments is shown in Fig. 8*A*. The time course of recovery was determined by plotting the ATP response amplitude against time elapsed since the removal of PPADS and fitting the data with a single exponential curve (Fig. 8*B*). This analysis yielded time constants of 1.4 ± 0.2, 2.0 ± 0.2, and 3.0 ± 0.3 min for 1, 1.5, and 2.5 μM PPADS, respectively.

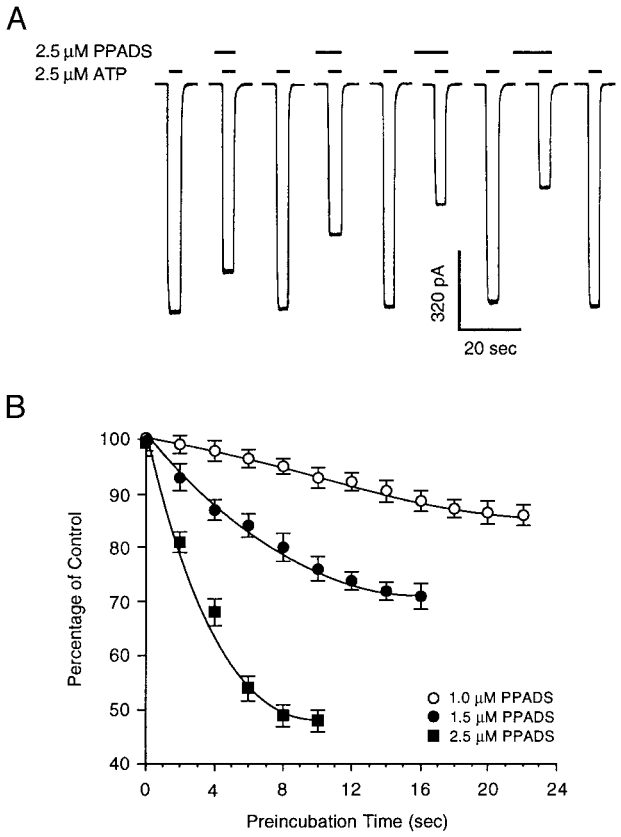

FIG. 7. Time course of inhibition of ATP-activated current by PPADS in the absence of agonist. *A*: records of current activated by 2.5 μM ATP and their inhibition by 2.5 μM PPADS preapplied for (from left to right) 2, 4, 6, and 8 s. Records are sequential current traces obtained from a single cell. Note that increasing the preapplication time increased the magnitude of inhibition of ATP-activated current by PPADS. *B*: graph plotting percentage of control response of 2.5 μM ATP-activated current as a function of preincubation time for 1.0 (○), 1.5 (●), and 2.5 (■) μM PPADS, respectively. Fitting the data to a single exponential decay yielded time constants of 16.4 ± 4.5, 9.2 ± 1.7, and 2.9 ± 1.5 s for 1, 1.5, and 2.5 μM PPADS, respectively.

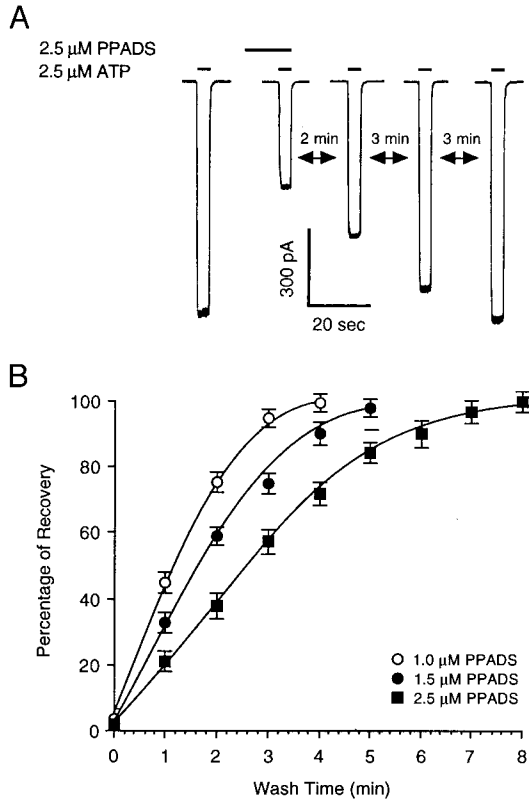

FIG. 8. Time course of slow recovery from inhibition of ATP-activated current by PPADS. *A*: records of current activated by 2.5 μM ATP in the absence and the presence of 2.5 μM PPADS. PPADS was preapplied for 10 s, and recovery of ATP-activated current from PPADS inhibition was complete after 8 min. *B*: graph plotting percentage recovery of 2.5 μM ATP-activated current as a function of wash time for 1.0 (○), 1.5 (●), and 2.5 (■) μM PPADS, respectively. Percentage recovery was calculated as: % recovery = $[(I_{test} - I_{inhibited})/(I_{control} - I_{inhibited})] \cdot 100$, where I_{test} is the peak of the test response after PPADS application, $I_{inhibited}$ is the peak of ATP response in the presence of PPADS, and $I_{control}$ is the peak of ATP response before PPADS application. Fitting the data to a single exponential function yielded time constants of 1.4 ± 0.2, 2.0 ± 0.2, and 3.0 ± 0.3 min for 1, 1.5, and 2.5 μM PPADS, respectively. PPADS was preapplied for 22, 16, and 10 s for 1.0, 1.5, and 2.5 μM respectively.

Time course of PPADS dissociation from ATP-gated ion channels in the absence of agonist

To examine the rate of dissociation of PPADS from ATP-gated ion channels in the absence of agonist, 2.5 μM PPADS was applied for 10 s in the absence of agonist, the cell was superfused with normal extracellular solution for a variable time interval to allow for dissociation of PPADS in the absence of ATP, and then 2.5 μM ATP was applied. The initial amplitude of the resulting current was taken as an indication of the degree of occupancy of the receptor-channel by PPADS in the absence of ATP. The traces in Fig. 9*A* show that increasing the length of the wash interval between application of PPADS and that of ATP resulted in a decrease in the degree of inhibition by

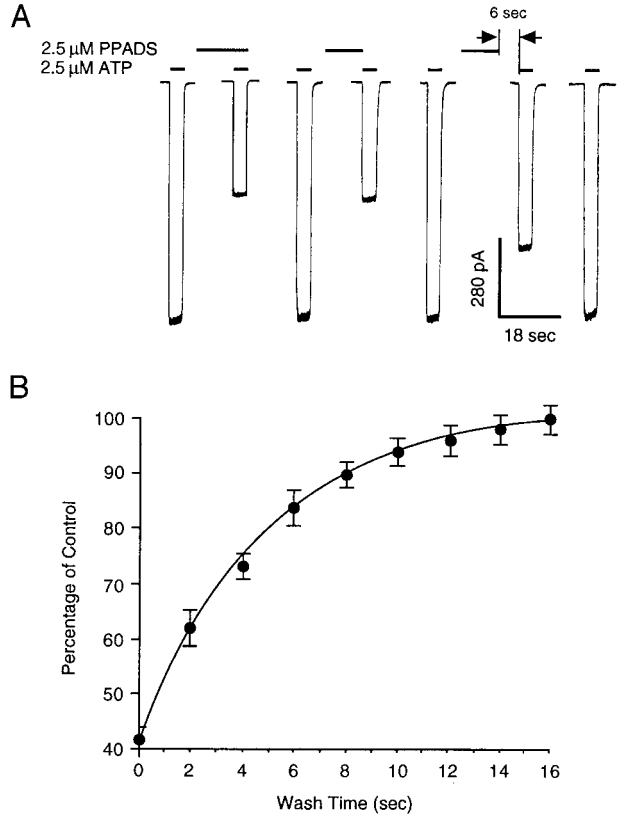

FIG. 9. Time course of PPADS dissociation from ATP-gated ion channels in the absence of agonist. *A*: records of currents activated by 2.5 μM ATP and their inhibition by 2.5 μM PPADS preapplied for 10 s, followed by a wash interval of varying duration before application of ATP in the absence of PPADS. Note that increasing the length of the wash interval between application of PPADS and that of ATP resulted in a decrease in the degree of inhibition by PPADS. *B*: graph plotting percentage of control response of 2.5 μM ATP-activated current as a function of the duration of the wash interval for 2.5 μM PPADS. Fitting the data to a single exponential function yielded a time constant of 3.4 $\pm$ 1.5 s for 2.5 μM PPADS. PPADS was preapplied for 10 s.

PPADS. On average, a single exponential fit of the plot of percentage of control ATP-activated current versus the length of the wash interval yielded a time constant for PPADS dissociation in the absence of agonist of 3.4 $\pm$ 1.5 s. This rate of offset of block by 2.5 μM PPADS was much slower than those observed for all concentrations of PPADS in the presence of ATP (Fig. 4*C*).

DISCUSSION

Bullfrog DRG neurons are known to possess P2X receptors, and activation of these receptors produces an inward ion current (Bean 1990; Bean et al. 1990; Li et al. 1997a,b). The results reported here show that the inward current activated by ATP in bullfrog DRG neurons was inhibited by PPADS. The inhibition was concentration-dependent over the concentration range 0.5–10 μM, and the 50% inhibitory concentration (IC_{50}) of PPADS was 2.5 μM. In addition, the PPADS concentration-response curve had a Hill coefficient of 1.8, which is significantly different from unity, suggesting that there is more than one binding site for PPADS and cooperativity among these sites.

In the present study, PPADS acted as a noncompetitive antagonist of ATP, as it significantly decreased the E_{max}, but did not alter the EC_{50} or slope factors of the ATP concentration response curve. In noncompetitive inhibition, the antagonist binds to an allosteric site on the receptor while agonist is bound and may act by any of a number of mechanisms, including open-channel block (also referred to as uncompetitive inhibition) and enhancement of desensitization. An action of PPADS to increase receptor desensitization could be largely excluded in the present study based on the observation that PPADS did not change the decay rate of ATP-activated current when PPADS was applied before application of ATP. In addition, increasing receptor desensitization by elevating the ATP concentration did not alter the inhibitory effect of PPADS. The possibility that PPADS acts via open-channel block was evaluated by testing whether the inhibition was voltage dependent; it was found that PPADS inhibition of ATP-activated current was independent of membrane voltage between -80 and $+40$ mV. This would not rule out the possibility of an open-channel block mechanism, however, as PPADS could bind to a site within the ion channel but beyond the influence of the membrane electrical field (Hille 1992; e.g., Marszalec and Narahashi 1993). However, evidence of agonist dependence generally is required to establish a channel-block mechanism of inhibition for slowly dissociating blocking agents using whole cell recording (Newland and Cull-Candy 1992). In the present study, the initial observation that the onset of inhibition by PPADS was relatively slow could be an indication of use dependence. When this possibility was evaluated using preapplication of PPADS in the absence of ATP, however, inhibition of peak and steady-state current did not differ. This observation indicates that PPADS association with its site of action on the ATP-gated ion channel does not require channel activation, which is not consistent with a channel-block mechanism of inhibition, as channel-blocking agents can bind in the ion channel only in the open agonist-bound state (MacDonald et al. 1987). In addition, the initial observation of slow recovery from PPADS inhibition also could be an indication of use dependence, as many use-dependent blocking agents exhibit trapping within the ion channel upon channel closing and dissociate from their binding sites much more rapidly when the channel is opened by the agonist (MacDonald et al. 1987). In the present study, the slow recovery from PPADS inhibition occurred in the absence of ATP. Although this finding could be explained by a "leak" exit pathway for PPADS when the blocker is trapped in the unliganded closed channel (Hille 1992), the observation that agonist application does not enhance the recovery from inhibition makes a trapping action highly improbable. Thus PPADS does not appear to act by blocking the open ATP-gated ion channel. The kinetics of inhibition of PPADS also supports this conclusion. Additional evidence against use dependence is that the time constants of both onset (Fig. 4*B*) and offset (Fig. 4*C*) of PPADS inhibition are independent of agonist concentration. This observation could be explained by a noncompetitive mechanism of inhibition in which PPADS acts at an allosteric site on the ATP-gated receptor-channel outside of the ion channel pore.

Although it appears that PPADS does not act on the channel pore region of ATP-gated ion channels, the identity of the site of PPADS action is unclear in the present study. Patch-pipette perfusion experiments showed that an estimated intracellular concentration of ~9.5 μM PPADS, which produced nearly maximal inhibition when applied extracellularly, did not alter

the effect of PPADS applied externally. This suggests that the site of PPADS action is accessible from the extracellular region, rather than the cytoplasmic region, of the receptor-channel complex. This is in agreement with recent observations by Buell et al. (1996), who reported that PPADS interacted in part with a lysine residue in the extracellular region of mammalian recombinant P2X receptor subunits. The observation of the relatively slow onset of action of PPADS suggests that the drug reaches its site of action, or binds to its site of action, slowly. A similar slowly developing inhibition has been observed for PPADS inhibition of ATP-activated current in other preparations such as rat pelvic ganglion neurons (Zhong et al. 1998), and for reactive blue 2 inhibition of NMDA-gated channels in mouse hippocampal neurons (Peoples and Li 1998).

Although the slow rate of recovery of ATP-gated channels from PPADS inhibition was not attributable to recovery from open-channel block, this process was not completely independent of the state of the ion channel. This is evident from the marked discrepancy between the estimated dissociation rate of PPADS from unliganded ATP-gated channels (Fig. 9) and the observed slow rate of recovery of ATP-activated current from PPADS inhibition (Fig. 8). When PPADS was applied in the absence of agonist and then allowed to dissociate from the receptor-channels before application of ATP, the subsequent inhibitory effect of PPADS was reduced greatly compared with PPADS applied for an equivalent time followed immediately by PPADS in the presence of ATP. PPADS (2.5 μM) thus appeared to dissociate from unliganded P2X receptor-channels with a time constant of 3.4 s (Fig. 9*B*), whereas in the presence of ATP this time constant was increased to 3.0 min (Fig. 8*B*). Thus PPADS appears to be able to dissociate much more rapidly from channels that have not been activated by ATP than from those that have been activated. One possible mechanism that could explain this observation is that ATP-activated channels bind PPADS with significantly higher affinity, thus greatly decreasing the rate of PPADS dissociation from the receptor. Furthermore the dependence of the slow rate of recovery of ATP-gated channels from PPADS inhibition on PPADS concentration (Fig. 8*B*) suggests a complex process, such as the involvement of multiple, cooperative binding sites for PPADS. Further studies will be required to determine the precise mechanism responsible for these effects.

ATP can be released from damaged cells and activated platelets (Gordon 1986) as well as mast cells (Osipchuk and Cahalan 1992) in injured or inflamed tissue. As P2X receptors are present in afferent fibers of sensory neurons and presynaptic terminals (McCleskey and Gold 1999), locally released ATP may stimulate these sensory afferents. In addition, ATP enhances glutamate neurotransmission at sensory synapses in substantia gelatinosa of spinal cord slice (Li and Perl 1995), activation of presynaptic P2X receptors enhances glutamate release from sensory neurons in culture (Gu and MacDermott 1997), and P2X receptors mediate fast synaptic transmission in the dorsal horn of the spinal cord (Bardoni et al. 1997). Although the preceding studies indicate that P2X receptors are involved in nociceptive neurotransmission and neuromodulation, the absence of specific antagonists for P2X receptors has impeded determination of the precise roles of P2X receptors in these processes. At present, among commonly used P2 receptor antagonists, PPADS appears to be one of the most useful tools to study the role of these receptors in neuronal preparations. Although PPADS at high concentrations (>100 μM) can inhibit other types of ion channels, such as 5-HT_3 receptor-ion channels (unpublished observations), PPADS at lower concentrations (<100 μM) does not affect the function of several other neurotransmitter-gated receptors tested, including NMDA (Peoples and Li 1998), $GABA_A$ (unpublished observations), 5-HT_3 (unpublished observations), and nicotinic cholinergic (Zhou and Galligan 1996) receptor-ion channels. In addition, in intestinal smooth muscle, PPADS has been observed to inhibit P2X receptors much more potently than P2Y receptors (Windscheif et al. 1995). If this is also the case in neuronal preparations, PPADS could be useful in differentiating between P2X and P2Y receptor-mediated responses.

I thank Dr. Robert W. Peoples for helpful discussions, comments on the manuscript, and assistance with analysis; K. Xiong for assistance in preparation of figures; Dr. Thomas Lanthorn for helpful comments on the manuscript; and Dr. Forrest F. Weight for providing laboratory space and resources to perform these studies and for helpful comments on the manuscript.

Present address and address for reprint requests: Dept. of Lead Discovery, AstraZeneca, R and D Boston, Three Biotech, One Innovation Dr., Worcester, MA 01605.

Received 9 August 1999; accepted in final form 13 January 2000.

REFERENCES

ABBRACCHIO, M. P. AND BURNSTOCK, G. Purinoceptors: are there families of P2X and P2Y purinoceptors? *Pharmacol. Ther.* 64: 445–475, 1994.

BALCAR, V. J., DIAS, L. S., LI, Y., AND BENNETT, M. R. Inhibition of [^{3}H]CGP 39653 binding to NMDA receptors by a P_2 antagonist, suramin. *Neuroreport* 7: 69–72, 1995.

BARDONI, R., GOLDSTEIN, P. A., LEE, C. J., GU, J. G., AND MACDERMOTT, A. B. ATP P2X receptors mediate fast synaptic transmission in the dorsal horn of the rat spinal cord. *J. Neurosci.* 17: 5297–5304, 1997.

BEAN, B. P. ATP-activated channels in rat and bullfrog sensory neurons: concentration dependence and kinetics. *J. Neurosci.* 10: 1–10, 1990.

BEAN, B. P., WILLIAMS, C. A., AND CEELEN, P. W. ATP-activated channels in rat and bullfrog sensory neurons: current-voltage relation and single-channel behavior. *J. Neurosci.* 10: 11–19, 1990.

BROWN, C., TANNA, B., AND BOARDER, M. R. PPADS: an antagonist at endothelial P_{2Y}-purinoceptors but not P_{2U}-purinoceptors. *Br. J. Pharmacol.* 116: 2413–2416, 1995.

BUEL, G., LEWIS, S., COLLO, G., NORTH, R. A., AND SURPRENANT, A. An antagonist-insensitive P_{2X} receptor expressed in epithelia and brain. *EMBO J.* 15: 55–62, 1996.

BURNSTOCK, G. Purinergic nerves. *Pharmacol. Rev.* 24: 509–581, 1972.

BURNSTOCK, G. A basis for distinguishing two types of purinergic receptor. In: *Cell Membrane Receptors for Drugs and Hormones: A Multidisciplinary Approach*, edited by R. W. Straub and L. Bolis. New York: Raven, 1978, p. 107–118.

DELEAN, A., MUNSON, P. J., AND RODBARD, D. Simultaneous analysis of families of sigmoidal curves: application to bioassay, radioligand assay, and physiological dose-response curves. *Am. J. Physiol. Endocrinol. Metab.* 235: E97–E102, 1978.

DUNN, P. M. AND BLAKELEY, A.G.H. Suramin: a reversible P_2-purinoceptor antagonist in the mouse vas deferens. *Br. J. Pharmacol.* 93: 243–245, 1988.

FREDHOLM, B. B., ABBRACCHIO, M. P., BURNSTOCK, G., DALY, J. W., HARDEN, K. T., JACOBSON, K. A., LEFF, P., AND WILLIAMS, M. Nomenclature and classification of purinoceptors. *Pharmacol. Rev.* 46: 143–156, 1994.

FRÖHLICH, R., BOEHM, S., AND ILLES, P. Pharmacological characterization of P_2 purinoceptor types in rat locus coeruleus neurons. *Eur. J. Pharmacol.* 315: 255–261, 1996.

GORDON, J. L. Extracellular ATP effects, sources and fate. *Biochem. J.* 233: 309–319, 1986.

GU, J. G. AND MACDERMOTT, A. B. Activation of ATP P2X receptors elicits glutamate release from sensory neuron synapses. *Nature* 389: 749–753, 1997.

GU, X. AND SACKIN, H. Effect of pH on potassium and proton conductance in renal proximal tubule. *Am. J. Physiol. Renal Physiol.* 269: F289–F308, 1995.

HILLE, B. *Ionic Channels of Excitable Membranes.* Sunderland, MA: Sinauer, 1992.

KENNEDY, C. P_1- and P_2-purinoceptor subtypes—an update. *Arch. Int. Pharmacodyn.* 303: 30–50, 1990.

KENNEDY, C. AND LEFF, P. How should P_{2X} purinoceptors be classified pharmacologically? *Trends Pharmacol. Sci.* 16: 168–174, 1995.

KHAKH, B. S., HUMPHREY, P. P., AND SURPRENANT, A. Electrophysiological properties of P2X-purinoceptors in rat superior cervical, nodose and guinea-pig coeliac neurones. *J. Physiol. (Lond.)* 484: 385–395, 1995.

KHAKH, B. S., MICHEL, A. D., AND HUMPHREY, P.P.A. Estimates of antagonist affinities at P_{2X} purinoceptors in rat vas deferens. *Eur. J. Pharmacol.* 263: 301–309, 1994.

LAMBRECHT, G., FRIEBE, T., GRIMM, U., WINDSCHEIF, U., BUNGARDT, E., HILDEBRANDT, C., BÄUMERT, H. G., SPATZKÜMBEL, G., AND MUTSCHLER, E. PPADS, a novel functionally selective antagonist of P_2 purinoceptor-mediated responses. *Eur. J. Pharmacol.* 217: 217–219, 1992.

LI, C., PEOPLES, R. W., AND WEIGHT, F. F. Inhibition of ATP-activated current by zinc in dorsal root ganglion neurones of bullfrog. *J. Physiol. (Lond.)* 505: 641–653, 1997a.

LI, C., PEOPLES, R. W., AND WEIGHT, F. F. Enhancement of ATP-activated current by protons in dorsal root ganglion neurons. *Pflügers Arch.* 433: 446–454, 1997b.

LI, J. AND PERL, E. R. ATP modulation of synaptic transmission in the spinal substantia gelatinosa. *J. Neurosci.* 15: 3357–3365, 1995.

MACDONALD, J. F., MILJKOVIC, Z., AND PENNEFATHER, P. Use-dependent block of excitatory amino acid currents in cultured neurons by ketamine. *J. Neurophysiol.* 58: 251–266, 1987.

MARSZALEC, W. AND NARAHASHI, T. Use-dependent pentobarbital block of kainate and quisqualate currents. *Brain Res.* 608: 7–15, 1993.

MCCLESKEY, E. W. AND GOLD, M. S. Ion channels of nociception. *Annu. Rev. Physiol.* 61: 835–856, 1999.

MOTIN, L. AND BENNETT, M. R. Effect of P_2-purinoceptor antagonists on glutamatergic transmission in the rat hippocampus. *Br. J. Pharmacol.* 115: 1276–1280, 1995.

NAKAZAWA, K., INOUE, K., ITO, K., AND KOIZUMI, S. Inhibition by suramin and reactive blue 2 of GABA and glutamate receptor channels in rat hippocampal neurons. *Naunyn-Schmiedeberg's Arch. Pharmacol.* 351: 202–208, 1995.

NEWLAND, C. F. AND CULL-CANDY, S. G. On the mechanism of action of picrotoxin on GABA receptor channels in dissociated sympathetic neurones of rat. *J. Physiol. (Lond.)* 447: 191–213, 1992.

OSIPCHUK, Y. AND CAHALAN, M. Cell-to-cell spread of calcium signals mediated by ATP receptors in mast cells. *Nature* 359: 241–244, 1992.

PEOPLES, R. W. AND LI, C. Inhibition of NMDA-gated ion channels by the P2 purinoceptor antagonists suramin and reactive blue 2 in mouse hippocampal neurones. *Br. J. Pharmacol.* 124: 400–408, 1998.

PUSCH, M. AND NEHER, E. Rates of diffusional exchange between small cells and a measuring patch pipette. *Pflügers Arch.* 411: 204–211, 1988.

RALEVIC, V. AND BURNSTOCK, G. Receptors for purines and pyrimidines. *Pharmacol. Rev.* 50: 413–492, 1998.

TREZISE, D. J., KENNEDY, I., AND HUMPHREY, P.P.A. The use of antagonists to characterise the receptors mediating depolarization of the rat isolated vagus nerve by α,β-methylene ATP. *Br. J. Pharmacol.* 112: 282–288, 1994.

WINDSCHEIF, U., PFAFF, O., ZIGANSHIN, A. U., HOYLE, C.H.V., BÄUMERT, H. G., MUTSCHLER, E., BURNSTOCK, G., AND LAMBRECHT, G. Inhibitory action of PPADS on relaxant responses to adenine nucleotides or electrical field stimulation in guinea-pig taenia coli and rat duodenum. *Br. J. Pharmacol.* 115: 1509–1517, 1995.

ZHONG, Y., DUNN, P. M., XIANG, Z., BO, X., AND BURNSTOCK, G. Pharmacological and molecular characterization of P2X receptors in rat pelvic ganglion neurons. *Br. J. Pharmacol.* 125: 771–781, 1998.

ZHOU, X. AND GALLIGAN, J. J. P2X purinoceptors in cultured myenteric neurons of guinea-pig small intestine. *J. Physiol. (Lond.)* 496: 719–729, 1996.